Low Computational Sensing with Goertzel Filtering for Mobile Industrial IoT Devices

Jaswinder Lota[1], *Senior Member, IEEE* and Andreas Demosthenous[2], *Fellow, IEEE*
[1]*University of East London, London, UK,* j.lota@uel.ac.uk
[2]*University College London, London, UK.*

Abstract—**Internet-of Things (IoT) is getting connected to an increasing number of mobile devices such as autonomous vehicles, drones and robots. Termed as Mobile Industrial Internet-of Things (MI²oT) devices in this paper, a key requirement of these devices is to accurately estimate range and Doppler in various applications, in addition to data communication. Research efforts therefore include incorporating MI²-oT devices with high-data rate communications together with Frequency Modulated Continuous Wave Radar (FMCW) sensing capabilities. Range and Doppler sensing, in FMCW radars is undertaken by a two-stage Fast Fourier Transform (FFT) which is computationally demanding. It is challenging to design baseband processing with FFTs that can be implemented as low computational hardware or application specific integrated circuits (ASIC) in MI²-oT devices. This paper, presents a novel range and Doppler sensing technique based on Goertzel filtering, leading to considerable reduction in computations compared to the FFT. FMCW radar with Goertzel filtering and FFT are examined in three cases viz., sensing the range and velocity of a car, vibration and respiration monitoring. Simulation results show a computation reduction of the order of 6.3×, 7.7× and 8.1× inGiga-operations per second (GOPS) for the three cases respectively. The reduced computations increase the feasibility of implementing range and Doppler sensing in MI²oT devices which have restricted computational resources.**

Keywords—IoT, sensing, FFT, FMCW radar, Goertzel Filtering

I. INTRODUCTION

Internet-of Things (IoT) is being widely adopted at a fast pace globally with the mobile network connectivity offering many novel applications. Being enabled by various standards such as Narrowband IoT (NB-IoT) and Long-Term Evolution Machines (LTE-M), the number of devices connected to IoT continues to grow. This is forecasted to reach 4.1 billion by 2024, and is termed as Massive (M)-IoT. Future trend is however, towards increasing number of mobile devices being connected to the IoT; such as autonomous vehicles, including those deployed in industrial settings/warehousing for monitoring, drones and automated mobile robots. In this paper these are referred to the Mobile Industrial Internet of Things (MI²oT) devices. MI²oT device connectivity is regulated by the 3GPP 5G New Radio (NR) Release (Rel)-16/17 standard [1], which will support greater bandwidths to accommodate an ever-increasing number of these complex devices, with higher data transfer rates, high reliability and low latency applications. Apart from connectivity, sensing for accurate localisation will be a key requirement for MI²oT applications. Research efforts include incorporating high-data rate communications and high-resolution radar sensing capabilities operating in the millimetre wave frequencies. These two systems are preparing to share and reuse many common functionalities, such as steerable millimetre-wave antenna arrays. Motivated by this growing overlap, the vehicular community is already pursuing a vision of unified vehicular communications and radar sensing that represents a major paradigm shift for next-generation connected and self-driving cars. Frequency modulated continuous waveform (FMCW) radars offer a promising solution for localisation sensing in terms of low-power and low-cost implementation. Current efforts include developing suitable protocols such as Radar-Aware Carrier-Sense Multiple Access (RA-CSMA) to facilitate this unified approach [2]. Due to low-power technology in FMCW radar efforts are focussed towards reducing the cost of the radar front end, including CMOS implementations that enable tighter system integration [3], [4]. For range and Doppler sensing the FMCW radar employs a two stage Fast Fourier Transform (FFT) to develop a 2-D map of range and Doppler points which is power consuming [5], [6]. An optimized signal processor can reduce the size of the chip and complexity, resulting in lowering these requirements for the overall system [7]. However, designing baseband processing with reduced complexity FFTs leading to a low-computational hardware / (application specific integrated circuit) ASIC design [8] is challenging, as most M²IoT devices have limited computational resources.

This paper presents a novel range and Doppler sensing technique based on Goertzel filtering leading to considerable reduction is computation compared to the FFT. Reduced computations increase possibility of implementing low computation hardware/ASICs in MI²oT devices, rather than employing a FFT ASICs or a digital signal processors (DSP). Three cases viz., range and velocity sensing of a car, vibration and respiration monitoring are discussed. Section II details the signal processing flow for FMCW radar sensing, followed by Goertzel filtering for range and Doppler sensing. Section III details the simulation results for Goertzel filtering and FFT for the three cases. Results are analysed and computational reduction compared. Conclusions are in Section IV.

II. FFT AND GOERTZEL FILTERING

A. Signal processing flow for FMCW radar sensing

FMCW radars commonly use linear frequency modulation (LFM) for transmission in packets. Each packet consists of a series of LFM signals known as chirps. The chirp is reflected off the target and the radar receives the reflected signal. The delayed received signal is mixed with signal being transmitted resulting in a beat signal x_b, from which one can estimate the target range d, velocity v and in the case of stationary vibrating targets, the vibration frequency. The

frequency of x_b is known at the beat frequency f_b. The waveform of x_b with amplitude A and phase ϕ_b is given by:

$$x_b = A sin(2\pi f_b t + \phi_b) \qquad (1)$$

For LFM transmission with a given chirp ramp up rate (slope of the chirp) S the following can be derived [9]:

$$f_b = \frac{S2d}{c} \qquad (2)$$

$$\phi_b = \frac{4\pi v T_{sw}}{\lambda} \qquad (3)$$

$$\Delta\phi_b = \frac{4\pi\Delta d}{\lambda} \qquad (4)$$

where:
c : is the velocity of electromagnetic wave
T_{sw}: is the chirp duration/sweep time
λ : wavelength of transmission
$\Delta\phi_b$: is the change in ϕ_b due to a small change in range Δd

(2) and (3) are used to estimate d and v, while the time evolution of $\Delta\phi_b$ in (4) is used to estimate both amplitude and periodicity of vibration in case of a stationary target. The signal processing flow is shown in Fig. 1 where the first step is identification of the f_b frequencies from x_b. The f_b frequencies identified by the FFT correspond to target ranges, are known as the range FFT. When the distance to the target changes slightly from chirp to chirp within the packet, it results in changes of phase in f_b. With known phase changes the velocities of the targets or vibrations in case stationary targets, can be computed in the second set of tone identification slicing across the first layer of range FFTs. This second stage is termed as the Doppler FFT. A 2D map of velocity/phase and range points can be developed with further processing algorithms to consider noise. All range FFTs need to be processed and stacked for consecutive chirps, prior to employing Doppler FFT across the chirps. The range and Doppler FFT are the bulk of the signal processing computations. Conventional DSP processors usually have instructions and architecture features that accelerate the inner kernel of algorithms, so that FFT-typical butterfly operations are done efficiently. It is common for one Radix-2 butterfly to execute one cycle per point rate, which makes a N-point Radix-2 FFT implementations undertake $2Nlog_2(N)$ real multiplications.
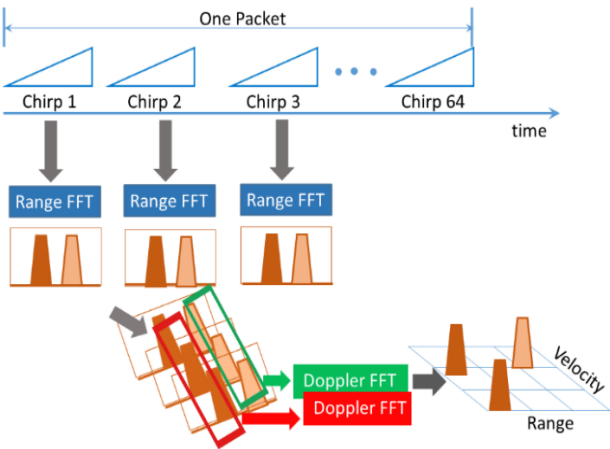
Fig. 1. FMCW radar sensing signal flow.

The FMCW radar model used in this paper is detailed in [10]. Typical FMCW radar parameters used are given in Table I.

B. Goertzel filtering range and Doppler sensing

Goertzel filtering is widely employed in dual-tone multi-frequency decoding and phase-shift keying/frequency-shift keying modem implementations, to compute DFT [11]-[14]. The Goertzel filter is computationally efficient and is implemented as a second-order Infinite-Impulse Response (IIR) filter as shown in Fig. 2.
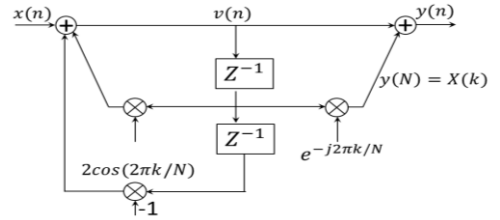
Fig. 2. Goertzel filter IIR implementation.

The z-domain transfer function of the Goertzel filter is:

$$H_G(z) = \frac{1 - e^{-j2\pi k/N} z^{-1}}{1 - 2\cos\left(\frac{2\pi k}{N}\right) z^{-1} + z^{-2}} \qquad (5)$$

where $2\pi k/N$ is the resonance centre frequency of the filter for N input samples. The time-domain difference equations for the Goertzel filter are:

$$v(n) = 2\cos\left(\frac{2\pi k}{N}\right)v(n-1) - v(n-2) + x(n) \qquad (6)$$

$$y(n) = v(n) - e^{-j2\pi k/N}v(n-1) \qquad (7)$$

To compute an N-point DFT (6) is implemented N times while (7) need be computed once after the arrival of the Nth input sample. Thus, for a real $x(n)$ the filter requires $N+2$ real multiplies and $2N+1$ real adds to compute an N-point DFT $X(k)$. Although the sweep bandwidth of the signal is 150 MHz, sampling must be at a rate that corresponds to the maximum beat frequency, which is less than the sweep bandwidth. The signal can be decimated to alleviate the hardware cost and run the ADC at the lower sampling rate.

For receivers, the received Signal Strength Indicator (RSSI) is used to detect the received power. This helps to provide the Automatic Gain Control (AGC) for the Low-noise Amplifier (LNA). The RSSI can be done at the RF/ IF signal, and can be analog or digital, e.g., RF Schottky envelope detectors can measure RSSI of signals from MHz to GHz range within an accuracy of $\pm$ 0.5 dB. The RSSI for the FMCW radar is given in Fig.3. Maximum sensing range of FMCW radar is 200 m and the range is sectioned into various zones. In Fig. 3 there are 20 zones, each zone covering a distance of 10 m. Each zone will have certain number of f_b,

that would be generated by x_b equal to the number of targets in that zone.
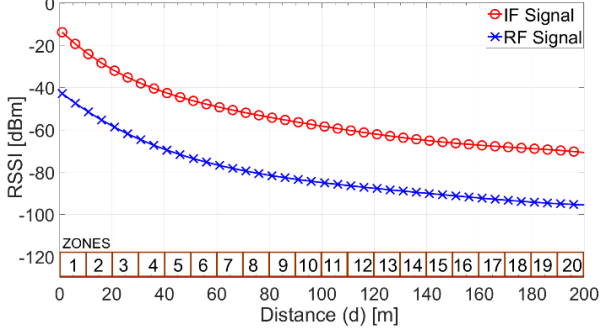
Fig. 3.   FMCW radar RSSI as a function of range.

Goertzel filter frequencies f_G are generated for each of the possible f_b for all zones to ensure all possible target locations from 1-200 m are covered. Frequency resolution f_0 of the FMCW radar in Table I is 1m. Each zone has eleven beat frequencies. The values of f_G and f_b for zone seven are indicated in TABLE II.

TABLE II.   GOERTZEL FILTER FREQUENCIES

Distance (d) m	Beat Frequency (f_b) MHz	$n = round\left[\dfrac{f_b}{f_o}\right]$	Goertzel Frequency $nf_0 = n\dfrac{f_s}{N}$ Hz
70	9.57	70	9.54
71	9.66	71	9.68
72	9.86	72	9.81
73	9.96	73	9.95
74	10.05	74	10.09
75	10.25	75	10.22
76	10.35	75	10.36
77	10.54	77	10.5
78	10.64	78	10.63
79	10.74	79	10.77
80	10.93	80	10.9

Goertzel filter frequencies can be similarly created for all zones. With the RSSI determined, Goertzel filtering is applied to only the set of 11 f_b frequencies for the zone where the target is likely to be present. There is no requirement of determining the beat frequency with the large sample set as in case of the range FFT. Once the beat frequency is determined, the phase variation in successive beat frequencies can be used to detect Doppler without the Doppler FFT. The flow diagram of the proposed technique is summarised in Fig. 4.
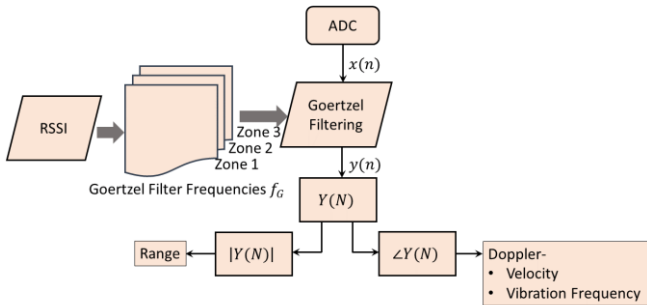
Fig. 4.   Low computation sensing with Goertzel filtering.

III.   SIMULATION RESULTS AND DISCUSSIONS

A. Car range and velocity detection

The MATLAB® 2018a simulation results for N =550 samples to detect two beat frequencies f_b = 9.57 MHz and 10.05 MHz that correspond to range detection of two cars A and B at 70 m and 74 m respectively are given in Fig. 5. The radar cross section (RCS) of the cars is assumed as given in [9]. The car A at 70 m is moving with a velocity of 220 km/h while the car B at 74 is assumed to be stationary. The results are compared to the standard FFT algorithm with 550 samples. It is seen that the Goertzel filtering can detect the beat frequencies with a resolution similar to the FFT algorithm. Both techniques lead to accurate range values of 70.14 m and 73.6 m for the two cars respectively.
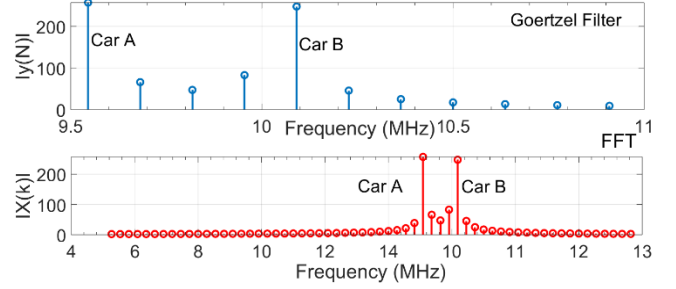
Fig. 5.   Car range detection with Goertzel filtering and FFT.

The required velocity resolution of the car is given by:

$$v_{res} = \frac{\lambda}{2N_c T_{sw}} \qquad (8)$$

From (8) a velocity resolution of ~ 1m/s will require N_c= 256 chirps. Phase difference ω measured across successive chirps obtained using Goertzel filtering and FFT together with the velocity of car A is shown in Fig. 6. With both techniques, a phase difference with a mean value of 1.51 is obtained from successive chirps, and the mean velocity estimated as 63 m/s or 226.8 km/h.
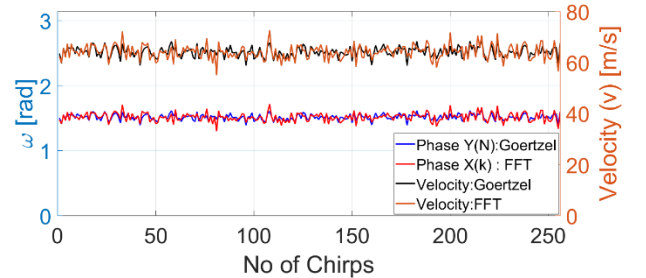
Fig. 6. Phase and velocity measurements with Goertzel filtering and FFT.

For range detection with Goertzel filtering, (6) requires only one real multiplication for each iteration. Since $N = 550$, the equation requires 550 real multiplications. Computing (7) requires multiplication of a complex number employing two real multiplications. Therefore, the total of real multiplications is 550+2 = 552 for each of the 11 Goertzel filter frequencies. For phase detection no real multiplications are required as the same is obtained from the phase of f_b.

B. Phase detection, vibration and respiration monitoring

Two examples of phase detection are given in this section, structural monitoring (e.g. vibrations at 1-50 Hz) and low (e.g. respiration at < 1 Hz) frequencies. These require different approaches. In both cases the range d =10.

a) Vibration: The RCS assumed of a target is that of a car [9]. The Goertzel filter generates a single tone corresponding to 1.367 MHz at 10 m. The vibrational frequency is sensitive to the change in phase of f_b from successive sweeps. The time evolution of phase can be used to estimate both the amplitude and periodicity of the vibration. The phase variation of successive chirps received for vibrations corresponding to a lateral periodic displacement of ±10 cm for the target is plotted for in Fig. 6. The phase variation indicates a time period T = 26.1 ms, corresponding to a vibration frequency of 38.3 Hz. The vibrational frequency accordingly can be determined with the Goertzel filter phase variations without the Doppler FFT. The number of chirps required to determine a single time-period N_c = 3560.
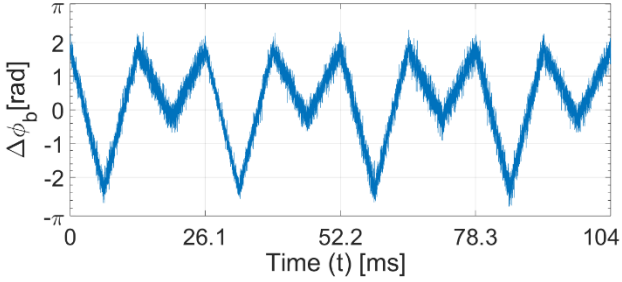
Fig. 6.   Vibration monitoring with Goertzel filtering.

b) Respiration: The main challenges are quantifying the RCS of physiological motion and isolating the contribution of respiration to the recorded power from other contributing factors such as the radar itself, antennas, propagation through the air and other reflectors in the scene. An ideal calibrated scenario is assumed for respiration movement of a lateral periodic displacement of 3 cm. The RCS assumed was for a human body at 10 m distance [9]. The phase values obtained from simulations are given in Fig 7. Typical frequencies are very low, which in this case is 0.38 Hz corresponding to 2.57 s of time-period for a normal breathing rate. A large value of N_c is required to measure this low frequency. which in this case is 350610.
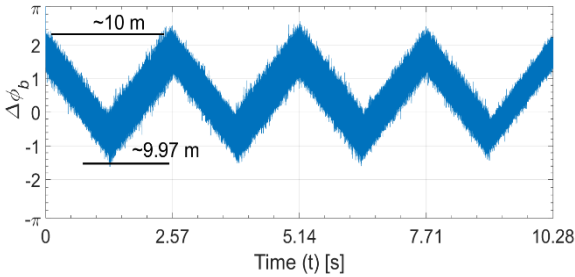
Fig. 7.   Respiration monitoring with Goertzel filtering.

C. Discussion

a) Car range and velocity with FFT: Firstly a FFT is applied along each linear sweep of the FMCW received signal with a frequency resolution of about $1/T_{sw}$= 136.36 kHz. For an input rate of 75 MHz this means an FFT of 550 samples. A power-of-two value of a 1024-point FFT is selected. The outputs of the first FFT are stored in a transpose RAM by row. For 256 chirps, the number of rows is taken as 256. A transpose memory of 256x1048 locations is required. Along the 1024 columns a 256-point FFT has to be applied and as a result a range-Doppler 256 x 1024 map is obtained where peaks along the rows reveal the distance of a target

while peaks along the columns reveal the speed of the target. The computational cost is due to the 1024-point FFT that has to be calculated for all the 256 rows and the 256-point FFT that has to be calculated for the 1024 columns. Only one channel FMCW radar is considered in this paper. FMCW radars can be multichannel and in such cases these operations must be repeated for each of the channels. Since the computational cost of each N-FFT for real multiplications is $2Nlog_2(N)$ then for all the FFTs in a single channel the number of real multiplications is:

$256 \times \{2 \times 1024 \times 10\} + 1024 \times \{2 \times 256 \times 8\} = 9437184$

b) Vibration monitoring with FFT: For vibration monitoring 3560 chirps are required which leads to a transpose memory of 4096×1024. Considering 3560 chirps would require a minimum 4096-point FFT (power of 2). In this case the number of real multiplications is:

$4096 \times \{2 \times 1024 \times 10\} + 1024 \times \{2 \times 4096 \times 12\} = 1.84 \times 10^8$.

c) Respiration monitoring with FFT: In the case of respiration the number of chirps is 350610. This results in a transpose memory of 524288×1024, as 350610 chirps would require a minimum 524288-point FFT (power of 2). The number of real multiplications is:

$524288 \times \{2 \times 1024 \times 10\} + 1024 \times \{2 \times 524288 \times 19\}$ $=3.1139 \times 10^{10}$

These need to be processed in a time slot of $N_c \times T_{sw}$ = 1.87 ms, 30 ms and 3.843 s for the three cases. For the car, vibration and respiration monitoring the computation for real multiplications is 5.04 Giga-operations per second (GOPS), 6.1 GOPS and 8.1 GOPS respectively.

d) Range, velocity, vibration and respiration monitoring with Goertzel filtering: For range 550 points are processed by filtering through the 11 Goertzel frequencies f_G depending on the zone indicated by the RSSI. At a given time only a specific zone is processed. The magnitude of the beat frequency obtained from Goertzel filtering determines the target range, while the phase difference and variation in successive chirps determines the car velocity, vibration and respiration rates. In all three cases phase estimation requires no real multiplications as there is no requirement of a Doppler FFT. Computation requirement for range is dependent on number of f_G in each zone, which is 11. The number of real multiplications   for detecting f_b is given by:

$N_c \times 11 \times (N + 2) = N_c \times 11 \times (550 + 2) = N_c 6072$.
These are to be processed in the time slots $N_c \times T_{sw}$, for all three cases. Computational requirement per second is given by:
$(N_c \times 6072)/(N_c \times T_{sw}) = 6072/T_{sw}$.

e) Computaion reduction: The Goertzel filtering computation depends on the number of samples required for range detection only. There is no additional computaion for velocity and phase detection. This results in 0.79 GOPS for all three cases. The reduced computation is 6.3×, 7.7× and 8.1× less than using the FFT for the range and velocity of car, vibration and respiration monitoring respectively.

IV.   CONCLUSIONS

Based on Goertzel filtering, the paper has presented a novel range and Doppler sensing technique with a substantially reduced computation as compared to the widely employed FFT. A single channel FMCW radar with Goertzel

filtering and FFT are applied to three cases viz., sensing range and velocity of a car, followed by vibration and respiration monitoring. Simulation results show a computation reduction of the order of 6.3×, 7.7× and 8.1×, in GOPS for the three cases respectively. The results can be extended to multichannel radars thus indicating further potential savings in terms of computation. The proposed technique is suitable for implementing in low-computation hardware/ASICs in MI²oT devices that are restricted in computation resources. Hardware implementation of the proposed technique is under way and will be detailed in a future publication.

REFERENCES

[1] 3GPP 5G NR Rel-16. Available on: https://www.3gpp.org/release-16

[2] V. Petrov, et al, "On unified vehicular communications and radar sensing in millimeter-wave and low terahertz bands," *IEEE Wireless Commun. Mag.*, vol. 26. no.2, pp. 146-153, Jun. 2019.

[3] A. Mostajeran, A. Cathelin and E. Afshari, "A 170-GHz fully integrated single-chip FMCW imaging radar with 3-D imaging capability,"*IEEE J. Solid-State Circuits,*, vol. 52., no.10, pp. 2721-2017, Oct. 2017.

[4] B. Ding et al., "A Ka band FMCW transceiver front-end with 2-GHz bandwidth in 65-nm CMOS," *IEEE Trans. Circuits Syst. II,* vol. 66. no.2, pp. 212-216, Feb. 2019.

[5] A. A. López et al., "Coherent signal processing for traffic flow measuring radar sensor," *IEEE Sensors J.*, vol. 18. no.2, pp. 4803-4813, Jun. 2018.

[6] H. Eugin et al, "Hardware architecture design and implementation for FMCW radar signal processing algorithm," in *Proc. Int. Design Archit., Signal Image Proc.,* Oct. 2014.

[7] T. Styles and L. Wildman, "An optimised processor for FMCW radar," in *Proc. 11th Radar European Conf. on Image Process.*, vol. 1, Oct. 2014, pp. 497-500.

[8] A. Ferizi et al, "An area-efficient 130 nm CMOS baseband processing unit for 24 GHz FMCW radar positioning," in *Proc. Int. Sym. Signal Syst., Electron., (ISSE)* Oct. 2012.

[9] C. Iovescu and S. Rao, "The fundamentals of millimeter wave sensros," Texas Instruments, May 2017. [Online]. Available: www.ti.com/lit/wp/spyy005/spyy005.pdf

[10] C. Karnfelt, C. et al, "77 GHz ACC radar simulation platform," in *Proc. IEEE Int. Conf. on Intell. Transp. Syst. Telecommun.*, (*ITST*), Oct. 2009.

[11] M. Felder, J. Mason, and B. Evans, "Efficient dualtone multi-frequency detection using the non-uniform discrete Fourier transform," *IEEE Signal Proces. Lett.*, vol. 5, pp. 160-163, July 1998.

[12] Using the ADSP-2100 Family, vol. 1. Norwood, MA: Analog Devices, 1995, chap. 14 [Online]. Available: http://www.analog.com/Analog_Root/static/library/dspManuals/Using_ADSP-2100_Vol1_books.html

[13] S. Gay, J. Hartung, and G. Smith, "Algorithms for multi-channel DTMF detection for the WERDSP32 family," in *Proc. IEEE Int. Conf. Acoust., Speech, Signal Process., (ASSP)*, 1989, pp. 1134-1137.

[14] K. Banks, "The Goertzel algorithm," *Embedded Syst. Programming Mag.*, pp. 34-42, Sept. 2002.